Observing protein interaction dynamics to chemically defined chromatin fibers by colocalization single-molecule fluorescence microscopy

[1]Maxime Mivelaz and [1]Beat Fierz*

[1] École Polytechnique Fédérale de Lausanne, SB ISIC LCBM, Station 6, CH-1015 Lausanne, Switzerland

*Corresponding author: beat.fierz@epfl.ch

Keywords: Transcription factor, HP1, chromatin structure, single-molecule fluorescence

Abstract

In eukaryotic cells, the genome is packaged into chromatin and exists in different states, ranging from open euchromatic regions to highly condensed heterochromatic regions. Chromatin states are highly dynamic and are organized by an interplay of histone post-translational modifications and effector proteins, both of which are central in the regulation of gene expression. For this, chromatin effector proteins must first search the nucleus for their targets, before binding and performing their role. A key question is how chromatin effector protein search, interact with and alter the different chromatin environments. Here we present a modular fluorescence based *in vitro* workflow to directly observe dynamic interactions of effector proteins with defined chromatin fibres, replicating different chromatin states. We discuss the design and creation of chromatin assemblies, the synthesis of modified histones, the fabrication of microchannels and the approach to data acquisition and analysis. All of this with the aim to better understanding the complex *in vivo* relationship between chromatin structure and gene expression.

1. Introduction

Chromatin effector proteins, including architectural proteins, histone modifying enzymes, gene repressive complexes, transcription activators and last, but not least, transcription factors (TFs) play a fundamental role in the regulation of gene expression in all cells. A detailed understanding of gene regulation thus requires knowledge how all these chromatin proteins search, interact with and shape the chromatin landscape.

Chromatin denotes the nucleic acid-protein complex, which organizes the eukaryotic genome. Nucleosomes, which form the fundamental unit of chromatin, are constituted of ~147 nucleic acid base pairs (bp) wrapped around a core of histone proteins (the canonical histones being H2A, H2B, H3 and H4) [1, 2]. Nucleosomes are not isolated particles but are arranged on genomic DNA in long arrays, interspaced by linker DNA of ~20 – 100 bps in length [3]. Nucleosomes can interact to form higher order structure, including local structural elements such as tetranucleosomal units [4] and extended fiber segments [5, 6]. Importantly, chromatin structure is highly dynamic, exhibiting structural motions in the milli-second to second time scales [7]. Structurally, the chromatin landscape is highly heterogeneous, with the presence of complex combinations of histone post-translational modifications (PTM) [8], histone variants and architectural proteins [9]. Histone PTMs provide binding platforms for a host of effector proteins, often equipped with combinations of PTM-specific "reader domains" to read-out the chromatin state [10, 11]. Finally, nucleosomes are constantly shifted, exchanged or disrupted by chromatin remodeling proteins [12, 13]. Currently, the detailed physico-chemical mechanisms of how combinatorial PTM signatures, effector proteins and structural features of the chromatin fiber itself dynamically interact are not well understood. A greater understanding of the complex interactions between all the factors involved in chromatin regulatory processes is of utmost importance, especially in light of the promise of therapies targeting chromatin signaling pathways.

Dynamic studies of how effector proteins read-out the chromatin landscape, by recognizing DNA motifs, histone PTM combinations or other structural features, are still scarce. In living cells, single-particle tracking of TFs has been successfully [14]. Recently, the dynamic behavior of chromatin regulatory complexes has been studied using similar methodologies [15-17]. These studies directly report on the behavior of proteins within their native environments. However, the chromatin substrate, with which they interact cannot be controlled or even probed. Detailed *in vitro* studies are highly complementary, as the chromatin state including the underlying DNA sequences can be tightly controlled. For dynamic studies, single-molecule methods have been especially attractive, as they provide direct access to mechanistic and physico-chemical parameters in a controlled system. Recent experiments have used single-molecule Förster Resonance Energy Transfer (FRET), or single-molecule

co-localization as readouts to detect binding dynamics of TFs [18-20] or chromatin effectors, including heterochromatin protein 1 (HP1) [21] or polycomb repressive complex 2 (PRC2) [22]. In the following, we will focus on such fluorescence based single-molecule techniques and provide details about experimental design principles, assembly of chemically defined modified chromatin, measurement parameters as well as data treatment to provide a primer for researchers interested in implementing such versatile assays in their laboratories.

To perform dynamic chromatin interaction experiments, e.g. to probe TF or histone PTM reader proteins, chemically defined chromatin fibers (e.g. containing a specific binding site as well as fluorophores for detection and a biotin moiety for immobilization) must first be assembled (**Fig 1a**). These steps might also require synthesis or semi-synthesis of modified histone proteins (**Fig 1b**).

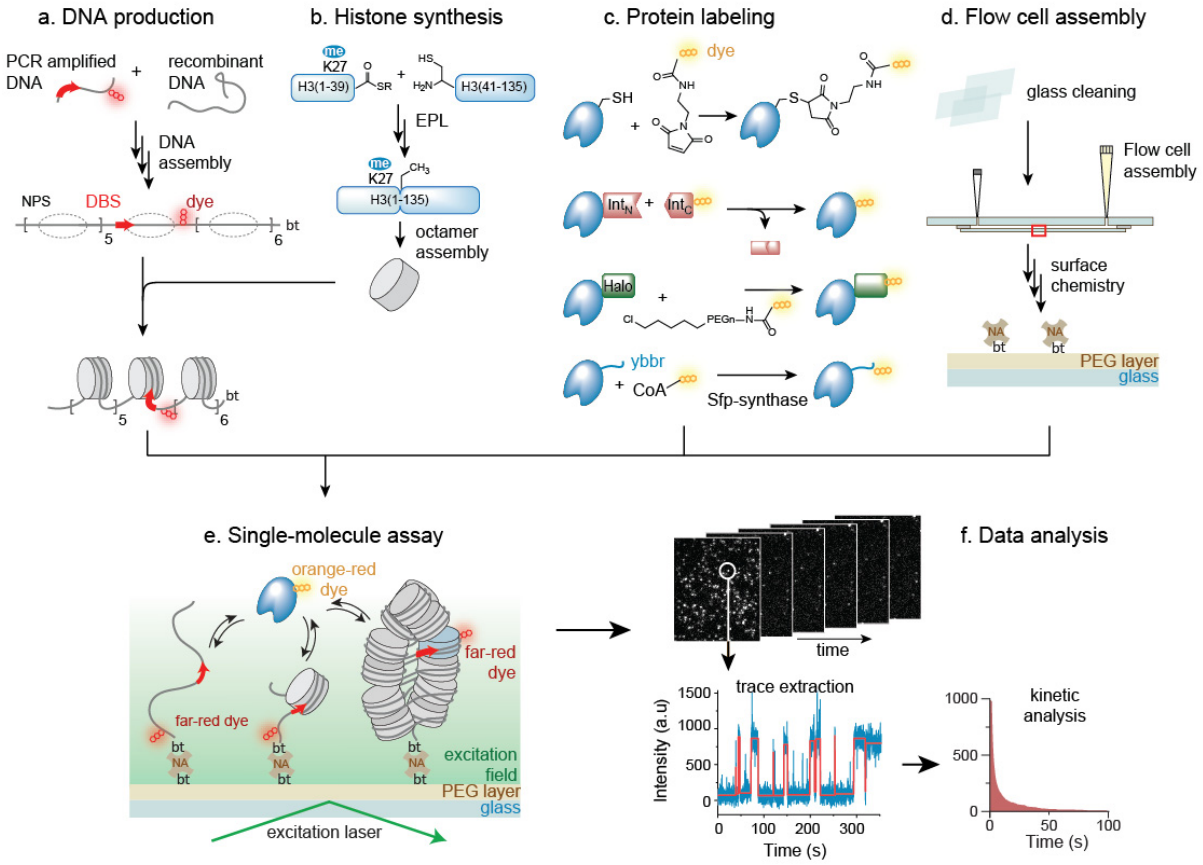

Figure 1: Overview over a single-molecule colocalization experiment to measure chromatin interaction dynamics. *Setting up this experiment requires* ***a.*** *production of chromatin DNA and* ***b.*** *modified histones to generate reconstituted chromatin fibers.* ***c.*** *Effector proteins, i.e. readers, remodelers or TFs have to be fluorescently labeled. After injection of all components into* ***d.*** *Flow cells,* ***e.*** *measurements can proceed, e.g. in a total internal reflection fluorescence (TIRF) setup, followed by* ***f.*** *Data treatment and kinetic analysis.*

Conversely, the proteins which are to be investigated have to be fluorescently labeled to enable detection of their binding kinetics (**Fig. 1c**). A wide variety of labeling methods are available, which enable defined, high efficiency labeling without disturbing protein function. For measurements, flow

cells with microchannels are required (**Fig. 1d**). Individual fluorescent chromatin fibers (or naked DNA / individual nucleosomes) are subsequently immobilized, followed by injection of fluorescently labeled effector proteins whose chromatin interaction dynamics (i.e. the colocalization of chromatin and protein signals over time) can be directly observed utilizing total internal reflection (TIRF) microscopy. Finally, binding events are characterized using a semi-automated approach which allows the identification of individual chromatin fibers and the extraction of binding data (**Fig. 1e**). The strengths and weaknesses of this fluorescence based *in vitro* approach are also discussed and we share our perspective on future avenues of research.

2. Single-molecule imaging of effector-chromatin interactions

In the following, we will provide a step by step overview for setting up single-molecule investigations of effector-chromatin interaction dynamics using a TIRF colocalization approach, following the outline provided in **Fig. 1**. We will start with DNA production and chromatin assembly using modified histones, then discuss setting up measurements, data acquirement and finally data analysis. This information can then serve as a primer to establish similar experimental systems.

2.1 Assembly of chromatin fibers

The advantage of performing *in vitro* studies on chromatin interaction dynamics lies in the fact that the chromatin state can be tightly controlled. A first prerequisite is thus to decide on the type and structural nature of the employed chromatin substrate. This includes the employed DNA sequence (potentially including nucleosome positioning sequences, NPS, and specific sequence motifs), the overall length (i.e. how many nucleosomes will be included) and the presence of markers, e.g. fluorophores. These decisions also determine DNA purification and assembly strategies. Moreover, histone subtypes and potential modification patterns have to be chosen. Finally, chromatin has to be reconstituted from individual components. In the following, we will highlight strategies to generate the appropriate chromatin substrate, using the example of a TF binding experiment that requires a specific sequence motif engineered into the center of a 12-mer chromatin fiber.

2.1.1 Choice of DNA for chromatin reconstitution

The generation of defined chromatin fibers is generally achieved by utilizing a DNA template containing tandem repeats of NPS. Several NPS have been preferentially used for *in vitro* reconstitution of nucleosomes and chromatin fibers [23], including an α-satellite repeat sequence [2], the 5S-RNA coding sequence [24] or the 601 NPS developed by Widom et al. [25]. The advantage of these particular sequences compared to most genomic DNA, is their ability to form nucleosomes that

are positioned with base-pair (bp) precision [26]. This ability is based on the fact that certain DNA sequence features impede or aid nucleosome formation [25-27]. Sequences with A/T dinucleotides in 10 bp periodicity facilitate DNA bending and are enriched in nucleosomal DNA *in vivo* [13, 28]. Conversely, homopolymeric DNA sequences are stiff and hinder the formation of nucleosomes *in vivo* and *in vitro* [29, 30]. In the case of the Widom 601 sequence, it has been shown that DNA-histone interactions are strongest at the midpoint of the NPS (where the nucleosome dyad axis intersects with the DNA) and that they are not evenly distributed along the DNA sequence [31, 32]. This heterogeneity may be an important factor to consider when planning *in vitro* assays using Widom 601, as DNA unwrapping rates may be different on either side of the nucleosome [33]. To reduce this heterogeneity, a palindromic sequence such as the α-satellite sequence or a palindromic version of the Widom 601 sequence may be used. The critical advantage of using NPS such as Widom 601 when designing an experiment is that they provide high spatial control of chromatin assembly. This enables the reconstitution of defined fibers with homogenous nucleosomal spacing [34], the precise placement of fluorophores [7, 35] as well as the integration of DNA sequence motifs at distinct positions.

2.1.2 Production of designer chromatin DNA

The generation of DNA sequences containing tandem repeats of NPS on a preparative scale is not straight-forward. In particular, if fluorophores or specific DNA sequence elements have to be installed at precise positions within the NPS arrays. Methods that allow the integration of individual fluorophores or DNA modification are based either on the replacement of short stretches of ssDNA [36], or on a modular system of individually modified DNA [7] or even chromatin segments [37].

We have developed a 5-piece modular method to generate chromatin DNA containing 12 601 NPS and two highly positioned FRET dyes at defined sites. The DNA was generated from two recombinantly derived pieces (containing 4 x 601 NPS and 5 x 601 NPS respectively) and 3 PCR generated pieces (each 1 x 601 NPS) [7]. The PCR generated pieces allow for the facile insertion of dyes and/or specific DNA sequence motifs into the central tetranucleosome unit of the chromatin fiber. The method relies on the generation of matching non-palindromic overhangs by restriction enzymes such as *BsaI* and *DraIII*, followed by sequential ligation steps. Importantly, the requirement of obtaining pure DNA fragments in high yield means that further purification steps by polyethylene glycol (PEG) induced precipitation are needed. Additionally, *ScaI* digestion sites were engineered between each 601 NPS to check chromatin array saturation after assembly.

If only a single internal nucleosome needs to be modified, the DNA ligation scheme can be simplified to a 3-segment ligation. In this case the specific modifications or DNA sequence motifs can

be inserted in the PCR produced nucleosome (piece no. 2, P2), which is then ligated to two flanking DNA segments (P1 and P3) that are produced in bacteria (**Fig. 2a**). Details of the method are found in section 4.1**.** In brief, the recombinant plasmids containing the 5 x and 6 x 601 Widom positioning repeats were cloned into a vector containing multiple *EcoRV* sites in its backbone (**Fig. 2b**). This facilitates purification of the insert from the backbone, by size-selective PEG precipitation. The plasmids are amplified in *E. coli* cell culture and purified by a large-scale alkaline lysis protocol. This purified plasmid DNA was further digested by *DraIII* (for P1) or *BsaI* (for P3), both of which are later digested with *EcoRV*.

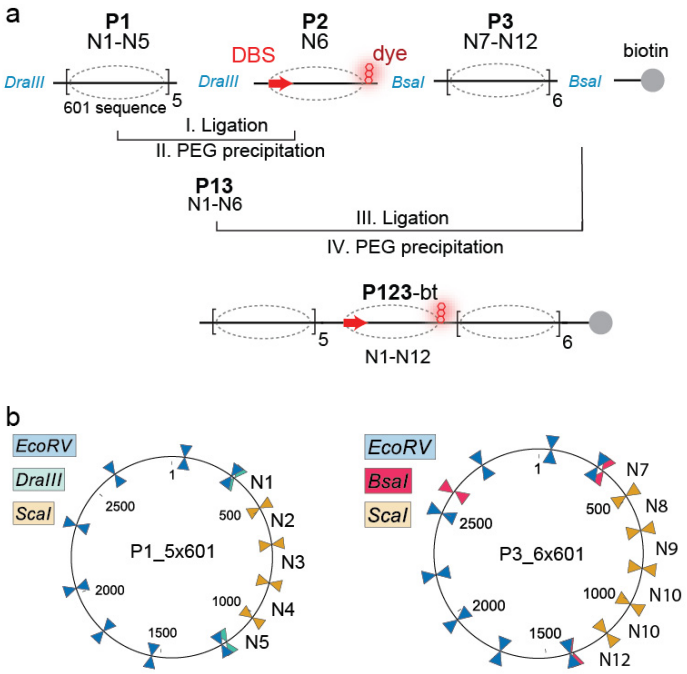

Figure 2: DNA design. a. *Sequential ligation strategy of recombinant pieces P1 and P3, as well as PCR produced piece P2, allowing to insert dyes or other specific DNA sequence into the center of a chromatin fiber DNA template. Matching restriction enzyme overhangs are indicated in blue. DBS: DNA binding site, e.g. of a TF.* ***b.*** *Design of bacterial expression vector to produce P1 and P2, and facilitate purification.*

For the PCR generated pieces, which can be modified and are flexible in sequence, templates e.g. containing 601 NPS or specific DNA motifs such a as TF binding motifs, are designed and cloned. Production of DNA is performed by PCR reactions, using synthetic primers and templates (96 individual 50 µL PCR reactions combined yield about 120-150 µg DNA). For dye labeling, we use PCR primers containing a modified oligonucleotide such as an amine-modified-thymidine which are reacted with an NHS-ester linked fluorophore, purified by HPLC and used in preparative, large scale PCR reactions. The choice of dye is important [38]. Ideally, dyes should be photostable (resistant to photobleaching), have low fluorescence intermittency (blinking), do not alter the physical properties of the substrate (polarity or charge) and they should have high extinction coefficients and quantum yields. A plethora of dyes have been used for *in vitro* imaging assays such as the Cyanine dyes (C3 or Cy5), Alexa Fluor

and ATTO dyes, all with various advantages and disadvantages [39]. We have extensively used ATTO 647N, Alexa Fluor 647, Alexa Fluor 568, Cy3B as well as Alexa Fluor 488, as these dye have shown high photostability, which is required for long imaging times. Another dye, JF-549, has shown excellent characteristics as well [40].

After preparative PCR, the P2 DNA fragment is digested with the appropriate restriction enzymes (i.e. with *DraIII* and *BsaI*) and used for DNA ligations (**Fig. 3a**). Sequential ligation of P1 with P2, are followed by purification by PEG precipitation, and ligation to P3 (as well as to the biotin anchor, **Fig. 3b**). Finally, the product is purified by PEG precipitation, yielding a complete chromatin fiber DNA template, containing 12 tandem repeats of 601 NPS, as well as fluorophores and distinct sequence motifs (e.g. a centrally positioned TF binding site).

Alternatively, for large scale generation of modular 12 x 601 NPS DNA specific restriction sites for nickases can be integrated into a DNA template [36]. Enzymatic nicking then allows the removal of a single-stranded fragment within the template DNA, which can be replaced with a modified sequence (i.e. labelled with a fluorophore). This approach reduces the need for sequential digestions and ligations but requires re-cloning and re-purifying the DNA template when the sequence needs to be varied.

2.1.3 Production of modified histone proteins and octamer reconstitution

A critical advantage of *in vitro* chromatin experiments is the ability to introduce patterns of histone PTMs at desired sites. Key technologies that enable PTM introduction include the application of genetic code expansion techniques [41, 42] or alkylation of cysteine residues, generating close analogues of modified amino acids [43]. A further, highly versatile strategy is based on the total chemical synthesis of modified histones by native chemical ligation (NCL) [44], or their semi-synthesis by expressed protein ligation (EPL) [45]. In this method two polypeptides, one carrying a C-terminal thioester, the other an N-terminal cysteine, are ligated together in aqueous conditions, forming a native peptide bond. The cysteine residue at the ligation site can subsequently be desulfurized to alanine, if required [46, 47].

Semi-synthesis, i.e. the connection of a synthetic and a recombinantly expressed protein part, is highly suitable for chromatin applications. Thus, we have primarily employed EPL to produce a variety of modified histones, including for the production of H3 trimethylated at lysine 9 (H3K9me3) [21], ubiquitylated and phosphorylated H2A [48] or for the generation of building blocks to assemble asymmetrically modified nucleosomes [49]. To introduce a histone PTM into the N-terminal tail of a histone protein, several steps are required, described here for the synthesis of H3K9me3: First, a suitable dissection site in the histone, here H3, has to be identified at which the sequence is split

between the synthetic and recombinant parts. For H3K9me3, the sequence is best divided between glycine 14 and alanine 15 (**Fig. 1b**). H3(1-14) is then synthesized using solid-phase peptide synthesis, carrying a tri-methylated lysine at position 9. For ligation purposes, a C-terminal thioester is introduced, either directly during synthesis [50], post-cleavage [51] or directly before ligation reaction through the use peptide hydrazides [52]. We have mostly used the latter approach in the generation of modified histones for our purposes. The recombinant part of the protein H3, H3(15-135), carrying a cysteine at the N-terminus instead of the native alanine (A15C) is expressed as a fusion to SUMO protein. After SUMO removal, the protein is purified and ligated to the peptide under denaturing aqueous conditions (generally 6 M guanidinium hydrochloride and phosphate buffer, pH 8) in the presence of thiols as ligation catalysts. Here, trifluoroethanethiol [53] or methyl thioglycolate [54] has been proven highly useful, as these thiol additive enable radical-initiated desulfurization post synthesis [46] in the same pot. After desulfurization, the native H3 protein carrying the desired modification is purified and can be used for chromatin assembly (for a full protocol see section 4.5). Finally, the recombinant expression and purification of canonical, unmodified H2A, H2B, H3 and H4 as well as the reconstitution of octamers has been reviewed in great detail [55]. Briefly, a full set of histone proteins (either unmodified or containing PTMs) are refolded into histone octamers by dialysis from 6 M guanidinium hydrochloride to 2 M NaCl containing buffer and purified by size exclusion chromatography. The reconstituted octamers are then directly used for chromatin formation.

2.1.4 Chromatin fiber reconstitution

In vitro assembly of chromatin fibres saturated with nucleosomes is essential for reproducible measurements. Fibers that are under-saturated could present compaction defects or leave areas of naked DNA which present a different binding target environment for effector proteins that contain DNA binding domains. To mediate this, purified 12 x 601 NPS DNA (containing dyes and/or specifically positioned sequence features including TF binding sites, section **2.1.2**) and reconstituted wild-type human octamers (section **2.1.3**) are dialyzed from high salt (2 M) to low salt (0.2 M) over 16-18 h [56] in the presence of competitor DNA to ensure full nucleosome occupancy (**Fig. 3c**). Competitor DNA is usually chosen to contain an NPS with a lower affinity to histones compared to the NPS present on the target chromatin DNA (e.g. for chromatin based on the 601 NPS, a NPS derived from the 3' long-terminal repeats of the mouse mammary tumor virus (MMTV) has been proven useful [57]). After chromatin fiber assembly, excess histone octamers and buffer DNA can be separated from reconstituted chromatin fibers by precipitation of the latter upon addition of 2-4 mM Mg^{2+} [57]. As the quantification of both 12 x 601 NPS DNA and reconstituted octamers can be imprecise, the ratio

of array DNA to octamer has to be experimentally optimized to form saturated arrays. We include restriction enzyme sites (for a blunt cutter e.g. *ScaI*)

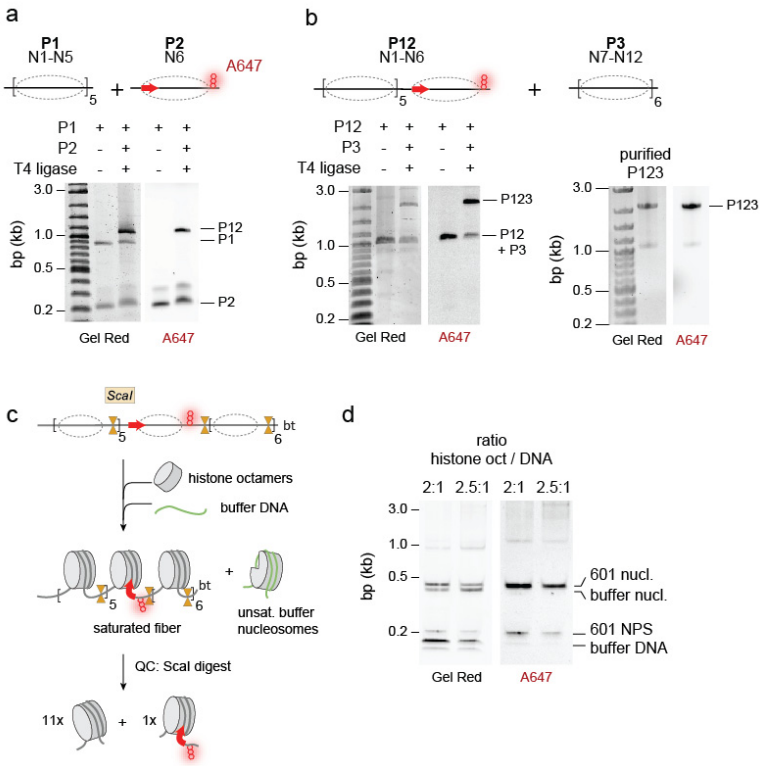

Figure 3: DNA and chromatin assembly. a. *First ligation between recombinant DNA segment P1 and PCR-produced DNA segment P2 (containing a TF target site: red arrow; and a fluorescent dye: Alexa Fluor 647, A647), producing ligated segment P12. Ligation progress is monitored by GelRed staining and A647 fluorescence.* ***b****. Second ligation between P12 and recombinant DNA segment P3.* ***c****. Strategy of chromatin assembly, using buffer DNA to ensure chromatin fiber saturation. QC: Quality control via restriction digest (using ScaI enzyme) to liberate individual nucleosomes.* ***d****. Analysis of restriction digest of chromatin fibers reconstituted using the indicated histone octamer:DNA ratios. In the optimal case, no fluorescent free DNA is observed, indicating full saturation.*

in between the NPS in our chromatin constructs (**Fig. 3c**). As a final quality control step, a small sample of reconstituted chromatin fibers are digested by *ScaI*. The resulting digestion mixture is analyzed using native gel electrophoresis (**Fig. 3d**). Fully saturated arrays release a homogenous population of nucleosomes with little remaining naked DNA [57].

The quality of the samples is of crucial importance for the success of any single-molecule experiment. Thus, appropriate analytics are critical to ensure that homogenous, saturated chromatin fibers (or nucleosomes) have been generated. While it is tempting to assemble only minute amounts of material (enough for subsequent single-molecule experiments), nevertheless all chromatin assembly protocols employed should generate enough material to enable biochemical controls and analysis using native gel electrophoresis. Finally, any impurities, in particular when fluorescent, have to be removed using appropriate purification schemes.

2.2 Protein Labelling

Having reconstituted chromatin in hand, the next step is the generation of fluorescently labeled effector protein (**Fig. 1c**), enabling the direct detection of chromatin interaction dynamics. An ideal labelling strategy is facile, robust, yields a single labeled species, and does not negatively affect protein function. For this the placement of the fluorescent label as well as the size of the modification (adduct, protein modification) must be considered.

The simplest strategy is the use of native or non-native cysteines on the surface of the protein of interest (POI). Cysteine labelling, e.g. using fluorophores carrying maleimide or iodoacetamide reactive groups, is facile and leaves a minimal scar. However, direct labeling methods are only applicable for POIs lacking native cysteines, which enables the inclusion of a positioned surface-exposed cysteine for labeling. Alternatively, there are a multitude of strategies available, of which we only highlight a few examples here: Enzymes have been widely used to label proteins [58]. Often, these methods require the integration of a short recognition sequence into the POI, which is recognized by an enzyme that covalently modifies the POI. These reactions are specific and can be done at low concentrations, however the short recognition sequence may leave a scar.

Self-splicing proteins such as inteins have been developed as a key resource for protein modification, including protein labelling [59]. These small amino acid sequences self fold into a conformation that favours the self-splicing reaction, excising themselves from a protein sequence. This reaction can be usurped to ligate a probe such as a dye to the C-terminus of a POI, with a minimal scar [21]. This selective reaction can be carried out at low concentrations. Finally, self-labelling tags, such as Halo, SNAP or CLIP, can be genetically encoded as fusion proteins [14, 60] and incubated with commercially available dyes. These self-labelling tags have the advantage of high labelling efficiency even at low concentrations, with the disadvantage of being large (~30 kDa for Halo).

The quality of the generated protein factors is of critical importance for the success of any single-molecule investigation. Indeed, in our experience the generation of highly pure, well behaved and uniformly labeled reader proteins or TFs can be a substantial challenge. Before employing them in single-molecule experiment, labeled proteins should be thoroughly characterized: Their homogeneity and oligomerization status has to be determined using size exclusion chromatography or similar experiments. Unless it is a critical feature of the protein under investigation, oligomerization can hamper subsequent experiments. Secondly, the labeling efficiency has to be assessed by performing careful UV-VIS spectroscopy. Finally, protein function has to be tested in ensemble experiments. Enzymes should be tested in appropriate assays to ensure their function and rule out any negative effects of the chosen labelling strategy. The chromatin or DNA binding properties of

reader proteins and TFs can be assessed using electrophoretic mobility shift assays (EMSA) or similar methods, again comparing labeled and unlabelled proteins. Only if a suitably robust protein production protocol has been established, subsequent single-molecule experiments become feasible.

2.3 Microchannel Fabrication

Binding experiments based on single-molecule fluorescence observation between chromatin and effector proteins, such as TFs or readers, are best performed within flow channels that enable tight control of reagent addition and oxygen exclusion. Careful cleaning and passivation all surfaces is vital to eliminate background fluorescence and non-specific protein adsorption during experiments. We perform experiments within flow cells (**Fig. 1d**) of approximately 120 µm height and a volume of about 20 – 30 µL, that are easily fabricated using a sandwich of microscopy slide and coverslip, spaced by double-sticky tape [38]. For surface cleaning, several techniques are available ranging from cleaning with KOH followed by flame treatment [61], HCL cleaning [62], plasma cleaning [63] and treatment with piranha etching [21] (**Fig. 4a**). Additionally, a passivation step avoiding unspecific interactions of DNA and proteins with the glass surface is required. Bovine serum albumin coating and a PEG brush have been previously described [64]. Both create a monolayer preventing contact with the glass surface. Finally, a tethering system to fix chromatin fibers to the glass surface must be used, i.e. employing anchoring molecules via the strong interaction between avidin and biotin [38].

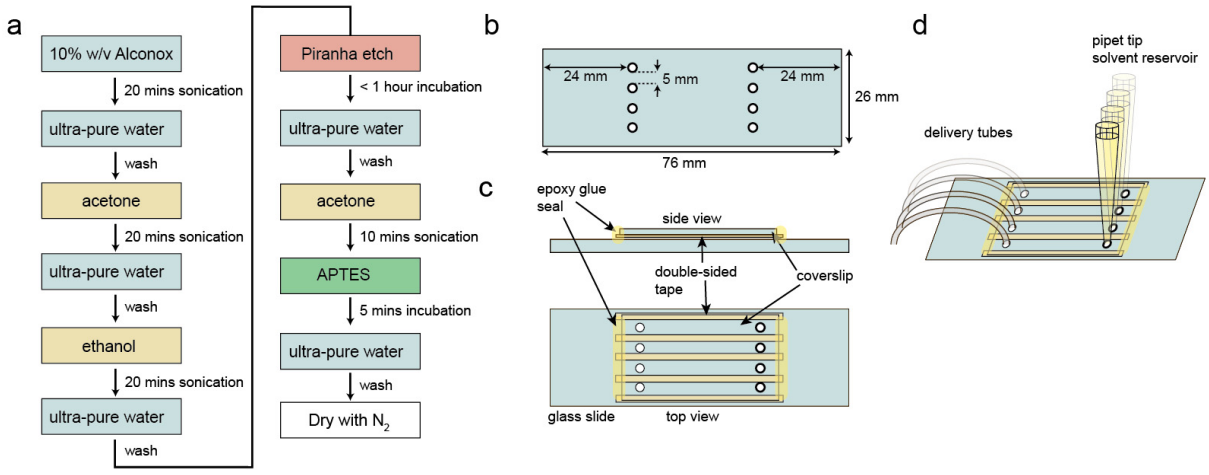

Figure 4: Microchannel assembly. a. *Workflow for glass cleaning and silanization, prior to channel assembly. APTES: (3-aminopropyl)triethoxysilane.* ***b****. Location of drilled holes in microscopy slide for the production of four flow channels.* ***c****. Final assembly of slide – coverslip sandwich, forming 4 flow channels.* ***d****. Final slide with connected tubes and solvent reservoirs.*

For our channel design, we drill a row of holes into glass slides (**Fig. 4b**) for solvent delivery. These pre-drilled slides, as well as TIRF-suitable coverslips are then thoroughly cleaned. We have found that utilizing piranha etching (a mixture of three parts concentrated H_2SO_4 to one part 30% aqueous H_2O_2 solution) provides the best results, in particular when accompanied by a cleaning

workflow including sonication in detergents and organic solvents (**Fig 4a**). After cleaning, both glass slides and coverslips are silanized in acetone using a suitable amino-silane, e.g. (3-aminopropyl) triethoxysilane (APTES). Silanized glass slides and coverslips are subsequently dried with inert gas and assembled into microchannels using strips of double-sided tape (**Fig. 4c**). In this state, the channels can be stored vacuum-wrapped in the freezer.

When required slide assemblies are defrosted and sealed with epoxy glue (**Fig. 4c**). Reservoirs consisting of plastic pipette tips are added to one side of the channels, and Teflon solvent delivery tubes are glued to the other (**Fig. 4d**). Then the channels surfaces are functionalized with a mixture of amine-reactive PEG and PEG-biotin [61], by injection of a 40:1 mix of NHS-PEG and NHS-PEG-biotin [61]. If required further passivation can be achieved by the addition of BSA to imaging buffers.

3.3 Data Acquisition

3.3.1 A general imaging protocol to observe chromatin binding kinetics

In general, single-molecule super resolution imaging requires the use of pure samples, buffers and a clean imaging surface. All this care is taken as to reduce the background fluorescence during image acquisition. In total internal reflection fluorescence (TIRF) microscopy [65] only a thin ~200 nm thick section of the specimen is illuminated by an evanescent field created at the site of laser reflection. Thus, only molecules within that volume are excited and visible, enabling the observation of single molecules up to a concentration of about 50 nM. For TIRF microscopy, we operate a Nikon Ti-E inverted microscope, equipped with a Nikon TIRF illuminator and a 100 x objective lens (CFI Apo TIRF 100 x Oil immersion objective, NA 1.49). The illumination is achieved using several laser lines (488, 532 and 640 nm, Coherent Obis) coupled into the system using an optical fiber and controlled via an accousto-optical tunable filter (AOTF). Fluorescence detection is achieved using appropriate band-pass filters and an electron multiplying charge coupled device (EMCCD) camera (e.g. Andor iXon 897).

To perform a chromatin binding experiment (**Fig. 5a**), we utilize the flow cells, prepared as described in the preceding chapter, and immobilize reconstituted chromatin fibers (e.g. containing a centrally positioned TF binding site) using avidin-biotin as an anchoring strategy. This places the fibers within the evanescent TIRF field. Moreover, as the chromatin fibers contain a fluorescent label (such as A647), we can directly detect the immobilized assemblies as diffraction limited spots in the field of view. We generally aim for 200 – 300 observable spots in a 25 – 50 µm imaging area, which enables clear discrimination between individual molecules. Using these observations in the far-red channel, the individual positions of each chromatin fiber can be determined using a spot-finding algorithm followed by a 2D-Gaussian fitting procedure.

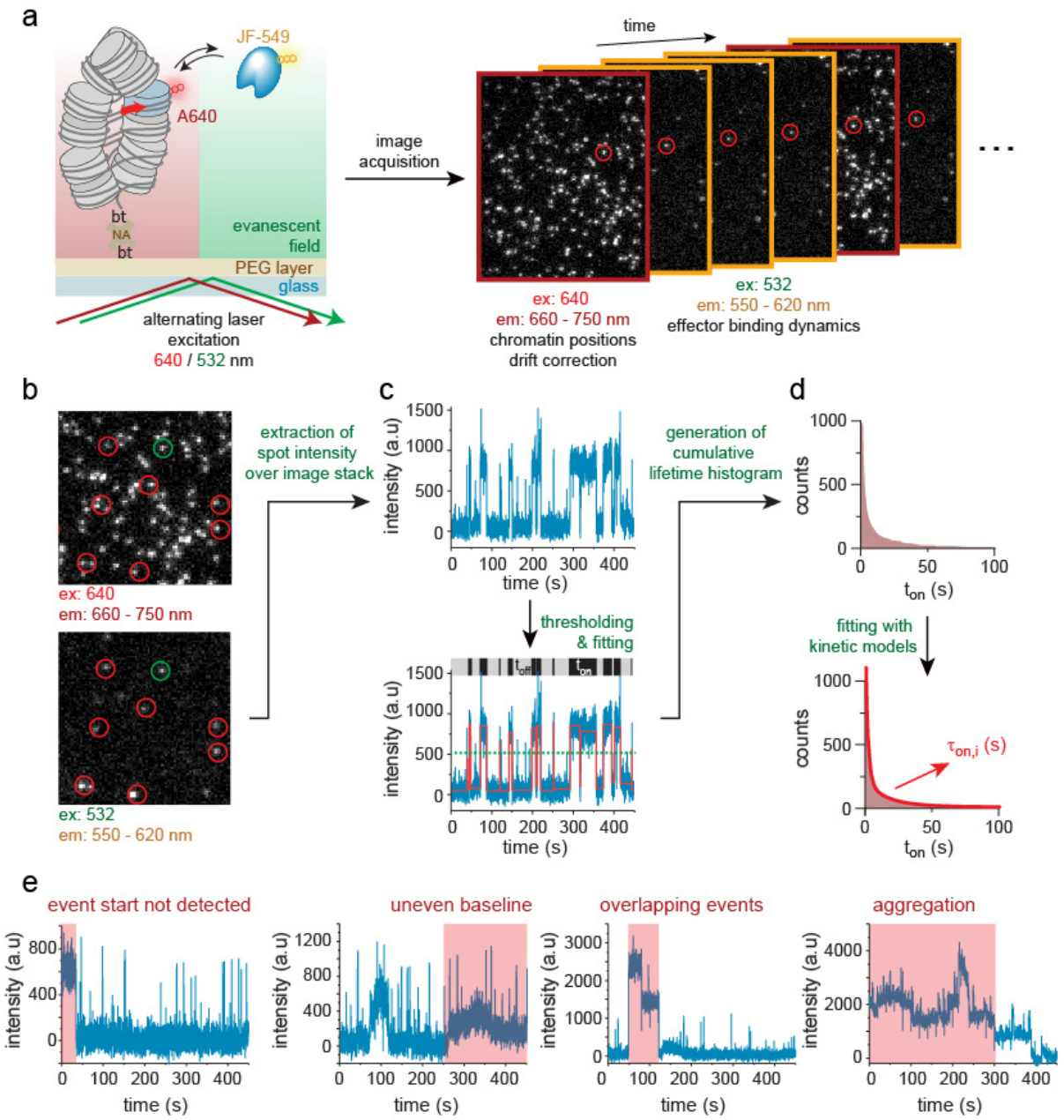

Figure 5: Data Acquisition. a. *Fluorescently labelled designer chromatin fibers are anchored onto the passivated and PEG functionalized glass surface using biotin. Red laser (640 nm) excitation illuminates attached fibers, whereas green laser (532 nm) illumination is employed to excite chromatin effector proteins that are within the evanescent field. Illumination using alternating red and green lasers allow fiber and effector localization over time.* ***b****. A single frame taken in the red and green laser channels highlights a subset of (red and green circles) chromatin fiber locations (640 nm illumination) which co-localize with a chromatin effector protein (532 nm illumination) at the time of imaging.* ***c****. Upper panel: For each determined chromatin spot (red and green circle) the intensity measured during green laser illumination (532 nm) is plotted as a function of time. Here is shown the example of the green circle in panel* ***b****. Lower panel: Using a semi-automated pipeline, the intensity-time plot is fitted and binding events above a fixed threshold can be extracted. The time a protein is bound (t_{on}) and the time intervals where no protein is bound (t_{off}) are determined for the entire trace.* ***d****. Once all bound and unbound time intervals are determined for individual traces, they are collated into cumulative lifetime histograms, which can be fitted to extract binding kinetics.* ***e****. Examples of kinetic traces with rejected events (red).*

Subsequently, fluorescently labeled effector proteins (reader proteins or TFs, carrying a label observable in the green-orange channel, such as ATTO532, Cy3B or JF-549) are injected into the flow

cell. Proteins, which enter the evanescent field and remain bound to chromatin for a sufficiently long time (usually in the tens of milliseconds time scale) generate a fluorescent signal upon illumination with the appropriate laser line, which can be detected. Exact spatial overlap of effector protein detections (in the green-orange channel) with chromatin fiber positions (in the far-red channel) indicates chromatin binding interactions. To detect binding dynamics, movies are recorded, using a frame rate significantly faster than the average binding event but slow enough to detect enough photons for a good signal-to-noise ratio. With a laser intensity of 20 W/cm^2 and an effective camera gain of 500, we generally use frame rates of 20 Hz to detect dynamic proteins, such as HP1, which exhibits residence times of > 150 ms [21]. For measurements that last several minutes, stage drift can become an issue. We thus record single frames in the far red channel (showing the position of chromatin templates) in regular intervals (**Fig. 5a**). These frames can be used for image alignment. Alternatively, fiducial markers, such as gold nanoparticles, can be used to align images over long timescales.

3.3.1 Optimization of imaging conditions

Fluorescence detection does not discriminate between molecules of interest that are specifically bound to a substrate or which are nonspecifically adsorbed to the surface. Nor does it distinguish between molecules of interest, fluorescent impurities attached to the glass or in the solvent, or carry-over from chemical reactions (such as labeling). As the accurate detection of single-molecules depends on a high signal to noise ratio, it is thus of critical importance to test the inherent background fluorescence within microchannels of the cleaned, silanized and PEG passivated slides in all the appropriate illumination wavelengths before starting any experiment. Defects in cleaning or passivation of glass surfaces are often the cause of high background. The quality of the passivation can further be determined by injecting a fluorescent protein into the channel (we have used labeled HP1α for this purpose). No more than 2-3 adsorbed molecules should remain in a 25 x 50 µm field of view [61]. Finally, all buffers and solvents need to be checked by imagining them in microchannels to see if they contain traces of fluorescent material.

The imaging buffers used in an experiment play an important role in establishing a physiologically relevant milieu for the biophysical and biochemical assays under investigation. Moreover, they are designed to improve the performance of the dyes used and to a lesser extent limit unspecific sticking to the glass surface. Controlling pH and salt concentrations (Na^+, K^+, Mg^{2+}) are essential as they influence not only the internal dynamics of nucleosomes and chromatin fibers [7, 57, 66], but they also influence protein-protein and protein-DNA interactions. Chromatin fiber

compaction is sensitive to salt concentrations, thus tight control over these parameters can increase reproducibility.

For optimal dye stability, enzymatic oxygen scavenging systems, such as glucose oxidase – catalase (GODCAT) or protocatechuate dioxygenase [67] are commonly added to imaging buffers. Importantly, dye blinking has to be avoided, as blinking events can be misinterpreted as dissociation events. Here, triplet quenchers are of great use [61, 68, 69], in particular 6-hydroxy-2,5,7,8-tetramethylchroman-2-carboxylic acid (Trolox), cyclopolyenes (cyclooctatetraene or COT) and nitrobenzoic alcohol (NBA), either as additive or even coupled to fluorophores [70]. The photophysical properties measured of a dye are environment specific [71] and their characterization is essential to distinguish real binding events from photophysical propensities. To this end, measuring the photobleaching and blinking rates of the selected dyes in the appropriate buffer system is essential to reduce misinterpretation of results. The selected dyes can be used to label modified DNA oligonucleotides containing a biotin moiety, which can then be immobilized in channels and imaged under continuous illumination using different laser intensities. From these measurements, dye lifetime kinetics can be determined using analysis principles as described below. For labelled proteins this bleaching rate can be measured by the adsorption of the protein on the passivated glass surface, although the proximity to the glass surface may induce an altered behavior of the dye. A more reliable method is to anchor the protein onto a passivated surface once again using biotin.

A final optimization step of the imaging system concerns the reduction of non-specific effector protein adsorption on the surface. Here, addition of detergents (e.g. 0.05% Tween or NP-40) as well as bovine serum albumin (BSA) to all buffers synergizes with PEG passivation to further reduce surface fouling.

3.3.3 Data analysis

Having all components in hand and having optimized the measurement conditions, a dynamic chromatin binding experiment, e.g. the binding of a transcription factor to immobilized chromatin fibers (**Fig. 5a**), can finally be performed. The data obtained from such an experiment, in the form of a movie with a set frame rate (e.g. 20 Hz) and an alternating sequence of excitation wavelengths has to be converted into an interpretable format. We have developed a series of ImageJ [72] and Matlab (Mathworks) scripts that simplify this task.

First, the individual images in the stack are corrected for background variation, e.g. using a rolling-ball algorithm. Second, chromatin fiber positions are identified (**Fig. 5b**). To this end, images recorded using laser excitation specific for the chromatin attached dye are analyzed (in our case, this is mostly the far-red channel). Using a peak-finding algorithm, individual spots indicating immobilized

chromatin fibers are detected. Using a 2D-Gaussian fitting algorithm, the point-spread function (PSF) of each diffraction limited spot is analyzed, the exact coordinates are extracted and saved. Performing this step over successive frames in the same channel (we generally record a far-red image every 200 frames) enables alignment of the whole image stack in case of weak stage drift (< 100 nm per 500 frames). Thirdly, fluorescence intensity time traces are extracted, by integration of the image intensity in each frame of the stack within a circle of a given pixel radius around the chromatin fiber position. The choice of radius depends on the signal density, the magnification and thus the detected point-spread function. In our instrument, which yields a 160 nm / pixel resolution, we generally integrate a 2 px radius for an optimal result.

Further steps are included to exclude contributions from fluorescent signals arising from nearby binding sites, or from fluorescence impurities not originating from single-molecules. 2D-Gaussian fitting of each detection above a given intensity threshold yields both coordinates and PSF shape parameters. Only fluorescence detected within a distance threshold (usually chosen as 200 nm, to allow for pixel fitting variations due to shot noise) and originating from a single-molecule (as judged by the PSF shape) are considered. Resulting from this data treatment, a fluorescence time trace for each chromatin position is obtained (**Fig. 5c**). If required, the resulting trace can further be filtered using an edge-preserving filter [73]. Applying either a simple thresholding algorithm or a more complex step detection algorithm [74], individual binding events are detected (**Fig. 5c**). This allows the subsequent extraction of times where the effector protein is chromatin-bound (t_{on}) and the time in between binding events (t_{off}). Cumulative histograms for both t_{on} and t_{off} are then analyzed using fitting to an appropriate kinetic model (**Fig. 5d**) to obtain kinetic constants. For simple binding reactions, a mono-exponential decay is usually sufficient, but more complex behavior might require multi-exponential analysis [21, 75]. Of note, an alternative approach is to employ hidden Markov models to directly interpret the observed binding pattern using a kinetic model [76]. The obtained kinetic constants, as well as the variation between individual chromatin fibers, potentially due to different mechanisms at play are the final result of the experiment and have to be interpreted within the biological context of the experiment.

Finally, not all binding events can be readily interpreted. Examples for fluorescent signals which are lacking information or are ambiguous are given in **Fig. 5e**. If possible, sample preparation and experimental conditions should be chosen such that overlapping binding events, aggregates or impurities leading to an unstable baseline are minimized. Individual ambiguous events have to be excluded from the analysis (as long as they do not represent a high percentage of all detections), which is achieved using semi-automated scripts, followed by manual inspection. This guarantees that generated kinetic curves actually represent real interaction kinetics.

3.3.4 Summary

Single-molecule imaging methods represent powerful tools to observe dynamic binding interactions of effector protein to chromatin fibers. Chemical control over individual components as well as assay environments, coupled with high time resolution, make co-localization single molecule fluorescence microscopy an ideal platform to study otherwise complex DNA-protein interactions. A key aspect of these experiments is the design and modular large-scale production of DNA templates containing distinct nucleosome positioning sequences, sequence motifs (such as TF binding motifs) and modifications, including fluorophores as well as their reconstitution into modified chromatin fibers. In this article, we have discussed several strategies that can be implemented to establish and streamline single-molecule workflows employing such designer chromatin to directly detect interaction dynamics. Paired with data analysis strategies, this chemical biology and biophysics toolbox can provide detailed insight into dynamic chromatin processes, from chromatin reader proteins, and transcription factors up to complex effectors, such as DNA repair or remodeling complexes.

4. Materials and methods

4.1 Large scale expression and purification of recombinant fragments

DNA fragments containing both 5 x 601 repeats (recP1) and 6 x 601 (recP3) repeats are cloned into a modified pWM530 vector using methods described previously [55] (**Fig 2b**). The inserts are designed as such that they are flanked by non-palindromic sequences recognized by restriction enzymes BsaI or DraIII.

1. Plasmids are transformed into DH5α (NEB, C2987) and large-scale (3 x 2 L) cultures in 2 x TY culture media (per 1L 16 g Tryptone, 10 g Yeast extract, 5 g NaCl) and left overnight (18-20 hours) shaking at 200 rpm 37 °C. Cell harvesting is done by centrifugation at 4’000 x rcf for 10 minutes at 4 °C (Beckman, JLA 8.100).

2. Alkaline cell lysis is then performed at room temperature according to published protocols [7, 55] by resuspending and combining all pellets in a total of 120 ml Alkaline Lysis solution I (50 mM Glucose, 25 mM Tris-HCl (pH 8.0), 10 mM EDTA (pH 8.0)) with the aid of a 10ml plastic pipette. Subsequent addition of 240 ml alkaline lysis solution II (0.2 M NaOH, 1% Sodium dodecyl sulfate (SDS)) is shaken vigorously and left to stand for 5 minutes. To neutralize the solution, 240 ml prechilled alkaline lysis buffer III (4 M Potassium Acetate, 2M Acetic Acid) is added and mixed by mild shaking.

3. After a further 15 minute incubation on ice the solution is centrifuged at 11'000 rcf for 10 minutes at 4 °C (Beckman, JLA 8.100), the supernatant is filtered through a miracloth (Merck, 475855) into a graduated cylinder. This sample is isopropanol precipitated using 0.52 volumes of isopropanol, mixed and left to stand at room temperature for 20 minutes. Nucleic acids are precipitated by centrifugation at 11'000 rcf for 10 minutes at 4 °C (Beckman, JLA 8.100). This should yield a substantial whiteish pellet which should be demarcated on the outside of the centrifugation tubes using a marker, as the pellet becomes translucent after drying.

4. Resuspension of the pellet is done using 30 ml TE 10 / 50 (10 mM Tris-HCl (pH 7.5), 50 mM EDTA) supplemented with 10 µl 100 mg / ml RNase A (Qiagen, 19101) and incubated at 37 °C for 2 hours. 5.2 g of KCl is directly added to the sample, dissolved and the solution is adjusted to 35 ml using TE 10 / 50. Centrifugation at 20'000 rcf for 10 minutes at 10 °C (Beckman, JA 12) clears the sample, allowing to purify the plasmid from the void volume using size exclusion chromatography on a FPLC (GE Lifesciences, ÄKTA pure).

5. The sample is loaded onto a 50 ml Superloop (GE Healthcare, 18-1113-82) and injected at 1 ml / min onto a XK 50 / 30 (GE Life Sciences, 28988953) column packed with 550 ml Sepharose 6 Fast Flow (GE Healthcare, 17015901) equilibrated with TE 10 / 50 supplemented with 2 M KCl (TEK 10 / 50). 12 ml fractions are collected from 0.2 column volumes (CV) until 0.5 CVs. Fractions containing the desired plasmid DNA are pooled and precipitated using 0.52 volumes isopropanol, 20'000 rcf for 10 minutes at 10 °C (Beckman, JA 12). Pellets are dissolved in TE 10 / 0.1 (10 mM Tris-HCl (pH 7.5), 0.1 mM EDTA) and stored at -20 °C.

4.2 Large scale enzymatic digestion and PEG purification of recombinant fragments

1. FPLC purified plasmids are first buffer exchanged by isopropanol precipitation and resuspended in ultra pure H_2O (Barnstead GenPure UF).

2. Typically, 100-150 pmol of plasmid is taken for digestion at 37 °C with either 200 units DraIII-HF (NEB, R3510) for recP1 or 200 units BsaI-HF (NEB, R3733) for recP3 in 1x Cutsmart buffer (NEB, B7204).

3. Digestion reactions are followed using 1 % agarose gels run at 100 V for 50 minutes in 1 x TBE until complete.

4. Subsequently, 100 units EcoRV-HF (NEB, R3195) are added to digest the plasmid backbone facilitating Polyethylene Glycol (PEG) precipitation purification. Digestion reactions are followed using 1 % agarose gels run at 100 V for 50 minutes in 1 x TBE until complete.

5. For PEG purifications a stock solution of 40 % PEG 6000 (Fluka, 81255) is used to make solutions of varying starting PEG concentrations, in 0.5 M NaCl and 10 mM Tris-HCl (pH 7.6). PEG acts like a crowding agent that can precipitate DNA fragments depending on their size, where lower PEG concentrations are required for larger DNA fragments. This purification technique can be difficult to setup as PEG %'s required for a particular fragment size depend on stock solutions and pipetting. In our hands we start with samples in PEG concentrations of 5 – 6 % in a total volume of 800 µl or more (this larger volume reduces pipetted errors due to PEGs viscosity). It is helpfully to keep an aliquot of the digestion to be used as an input to compare with purified pellets on gel before addition of PEG.

   5a. Samples are placed on ice for 20 minutes and then centrifuged at 20'000 rcf for 20 minutes at 4 °C.

   5b. Supernatants are placed into a fresh 1.5 ml microcentrifuge tube, pellets which may contain the DNA fragment of interest are kept on ice and 40 % PEG 6000 stock is added to the supernatant to increase by 0.5 % the total PEG concentration (NaCl concentration is adjusted accordingly to maintain 0.5 M).

   5c. The supernatant is placed on ice for 20 minutes and then centrifuged at 20'000 rcf for 20 minutes at 4 °C. And the process is repeated several times.

   5d. To check whether the fragment of interest has been purified out, pellets are resuspended in 50 µl 10 mM Tris-HCl (pH 7.6) and 0.5 µl loaded onto a 1 % agarose gel (a sample of the supernatant is also taken) run at 100 V for 50 minutes in 1 x TBE.

   5e. If the fragment remains in the supernatant continue to increase PEG concentrations. Usually samples containing the desired fragments are pooled and a second round of PEG purification is done again to increase purity. Finally, samples pooled and purified using QIAquick PCR purification spin column kits (Qiagen 28106) to remove excess PEG.

Troubleshooting

If no separation of the larger fragment compared to the smaller ones can be seen this may be due to:

1) Inadequate removal of supernatant (slow pipetting from the center of the tube is recommended).
2) Starting PEG concentration is too high or salt concentration is too high

4.3 Synthesis of Labelled DNA P3 Fragment

Fluorescently labelled fragments are obtained using previously described methods [6].

1. Primers of single stranded DNA containing internally amino modified C6 dT (Integrated DNA Technologies, IAmMC6T) are ordered and ethanol precipitated upon receipt and resuspended in ultra pure water (Barnstead GenPure UF).

2. 5 - 10 nmol of primer is diluted in 25 µl 0.1 M Sodium tetraborate pH 8.5 to which 5 µl of a 5 mM succinimidyl-ester modified Alexa 647 (Invitrogen, A20106) stock (in DMSO) is added. This coupling reaction is left mildly shaking in the dark at room temperature for 6 - 8 hours.

3. This reaction is followed by RP-HPLC on an InertSustain C-18 (GL Sciences, 5020-07445, 3 µm 4.6 x 150 mm) column using a gradient from 100 % solvent A (95 % 0.1 M triethylammonium acetate (TEAA) pH 7, 5 % ACN) to 100 % solvent B (70 % 0.1 M TEAA pH 7, 30 % ACN). Usually 0.4 µl of reaction is taken and resuspended in 49.6 µl of solvent A. If the reaction is not completed, an additional aliquot of dye is added. Completion depends on the dye used, in our hands this can range from 50 – 90 % labelling.

4. Upon completion, the reaction is ethanol precipitated twice in succession and finally resuspended in 100 µl solvent A. This sample is then purified using the same RP-HPLC method as above, both labelled and unlabeled primer are collected.

5. Samples are ethanol precipitated and dissolved in ultra pure water to a concentration of 2.5 µM ready for PCR.

4.4 Large scale formation of chromatin array DNA

Once fragments P1, P2 and P3 have been digested and purified, test ligations are performed to optimize conditions for complete ligation i.e P1 with P2 and P2 with P3. These optimizations allow to reduce the amount of unligated products and simplify the PEG purification steps. Typically, an excess of the PCR generated piece is used for the first ligation between P1 and P2 i.e 1 : 1.3 ratio of P1 : P2. This is because the difference in size between P1 and P12 is small, thus any remaining unligated P1 is harder to purify out. However, for the ligation of P1P2 with P3, an excess P3 (both constructs P1P2 and P3 are similar in size) as P1P2 is more difficult to generate.

1. P1P2 ligations are performed in 200 µl using optimized ratios of P1 to P2, in 1 x T4 Ligase buffer (NEB B0202) with 400 units of T4 ligase (NEB M0202). These reactions are usually left overnight at 37° C, after which a 1% agarose gel is run at 100 V for 50 minutes in 1 x TBE until all P1 has been ligated. If this is not the case more T4 ligase can be added as well as more P2 if required.
2. Upon complete P1 ligation, the P1P2 fragment is isolated via PEG precipitation described in section **4.2.5.** For fragments of this size a starting percentage of PEG from 5 – 6 % is recommended and PEG steps of 0.5 %. Pellets containing the desired fragments are pooled and purified using QIAquick PCR purification spin column kits (Qiagen 28106).

3. For the ligation between P1P2, P3 and biotin anchor the following ratio is used i.e 1 : 1.3 of P1P2 : P3 and 5x excess of biotin anchor. Ligations are performed in 200 µl with 1 x T4 Ligase buffer (NEB B0202) with 400 units of T4 ligase (NEB M0202). These reactions are usually left overnight at 37° C, after which a 1% agarose gel is run at 100 V for 50 minutes in 1 x TBE until all P1P2 has been ligated. If this is not the case more T4 ligase can be added as well as more P3 if required.

4. Upon complete ligation, the P1P2P3-bt fragment is isolated via PEG precipitation described in section **4.2.5.** For fragments of this size a starting percentage of PEG from 4 – 5 % is recommended using PEG steps of 0.3 %. Pellets containing the desired P123 fragments are pooled and purified using QIAquick PCR purification spin column kits (Qiagen 28106).

4.5 Semisynthesis of a histones

4.5.1 Automated Solid phase peptide synthesis

Here we provide a general histone semisynthesis protocol, based on the synthesis of H3K9me3. For this histone, the first 13 amino acids of histone H3 containing the desired modification (K9me3) were

synthesized as a C-terminal hydrazide (ARTKQTARKme3STGGK-hydrazide), using FMOC chemistry on a 2-Chlorotritly chloride resin (Cl-trt, Novabiochem, 855017) and using 2-(1H-benzotriazol-1-yl)-1,1,3,3-tetramethyluronium hexafluorophosphate (HBTU, Protein technologies) as coupling reagent.

1. The Cl-trt resin was preloaded with lysine-hydrazine by swelling 0.5 g (1 eq.) of resin in 3 ml DMF, followed by cooling to 0° C using an ice bath. A 1 ml solution of 3 eq. N,N-Diisopropylethlamine (DIEA) and 2 eq. hydrazine monohydrate in DMF is added dropwise and the suspension is stirred for 1 h at RT, after which 100 µl of methanol are added.

2. 5 eq. Fmoc-Lys-OH are dissolved in 0.5 M HBTU in DMF and reacted for 2 mins at RT. 10 eq. DIEA are added and reacted for 1 min at RT, followed by addition to the resin. After reacting for 30 mins, with occasional stirring, the resin is washed with DMF. The step is repeated with an additional 5. eq of activated amino acid. The resin is then washed with DCM, methanol and dried. Quantification of resin loading is done using UV-spectroscopy after deprotection using 20% (v/v) piperidine in DMF. The release of dibenzofulven (ε_{260} = 7800M^{-1} cm^{-1}) corresponding to the total amino acids on the resin.

3. Using an automated peptide synthesizer the remaining amino acids of the H3-tail are coupled to the prepared hydrazine resin, according to the manufacturer's protocol (we generally use HBTU chemistry). To increase synthesis yield, double coupling can be employed. We generally use the following protecting groups for given amino acids: Arg(Pbf), Lys(Boc), Thr(*t*Bu), Gln(Trt) and Ser(*t*Bu).

4. After synthesis, peptides are cleaved from the resin, using a cleavage cocktail of 2.5% H_2O, 2.5% Triisopropylsilane (TIS) and 95% Trifluoroacetic acid (TFA). After 1-3 hours of cleavage, the released peptide is precipitated by using cold diethylether and collected via centrifugation. The peptide is then purified using preparative HPLC.

4.5.2 Expression and purification of truncated H3 with C-terminal cysteine (H3Δ1-14)A15C

Expression and purification of C-terminal cysteine (H3Δ1-14)A15C was done as previously described [21]. Briefly, BL21(DE3) *E. coli* are transformed with a pET30 vector containing a His6-SUMO-H3Δ1-14(A15C) fusion insert. Following overnight expression, the protein of interest is isolated from inclusion bodies and purified using Ni-NTA affinity chromatography. Affinity tag cleavage is done using Ulp1 and the crude protein mixture is purified over RP-HPLC.

4.5.3 One-pot Ligation and desulfurization to generate H3K9me3

With purified peptide and protein in hand, the full-length, modified histone protein can be generated using expressed protein ligation [45].

1. Lyophilized peptide hydrazides are dissolved in ligation buffer (6 M Guanidinium hydrochloride (GuHCl), 0.2 M NaH_2PO_4, pH 3) at a concentration of 10 mM. This solution is cooled to -18°C in an ice/salt bath before the addition of 1.5 eq. of $NaNO_2$ from an aqueous 0.5 M stock. The reaction is left for 20 mins before adding 22.5 eq. of methyl thioglycolate (MTG) to form a thioester *in situ*. Using NaOH the pH is adjusted to 7 and the reaction is stirred at RT for 10 mins.

2. The MTG-peptide is added to a tube containing 0.33 eq of lyophilized protein, containing a N-terminal cysteine (H3Δ1-14)A15C. To this mixture, tris(2-carboxyethyl)phosphine (TCEP, buffered to pH 7) is added to a final concentration of 25 mM. The ligation reaction proceeds at 25° C for 16 h. The ligation progress is monitored by RP-HPLC and ESI-MS.

3. Upon completion of the reaction, the protein is desulfurized which reverts the cysteine at the ligation junction to alanine, regenerating the native H3 sequence. To this end, TCEP desulfurization buffer (0.5 M TCEP, 6 M GuHCl, 0.2 M phosphate, pH 7) is added to obtain a TCEP concentration of 0.25 M. A radical starter, 2,2'-Azobis[2-(2-imidazolin-2-yl)propane] Dihydrochloride (VA-044, Wako Chemicals, 017-19362) is added to a final concentration of 30 mM along with glutathione (GSH) (40 mM). The reaction proceeds at 30° C for 16 h. The reaction progress is followed by RP-HPLC and ESI-MS. Upon completion of the desulfurization, the final modified histone H3K9me3 is purified by semi-preparative RP-HPLC.

4.6 Dialysis reconstruction of 12x chromatin arrays

Purified P123-bt fragment (section **4.4**) and recombinantly expressed wild-type human octamers are dialyzed from high salt to low salt over 16-18 h.

1. 200 – 300 pM array DNA, 0.5 – 1 equivalents of MMTV (unspecific DNA used to gauge the saturation of chromatin arrays) and the experimentally determined ratio of DNA to octamers (start with 1 : 1, 1 : 1.5 and 1 : 2 DNA to octamer ratios) are added to a total volume of 20 µl

in TE buffer (10 mM Tris pH 7.5, 0,1 mM EDTA pH 8) containing 2M KCl. This sample is placed in preequibrilated micro-dialysis units (Thermo Scientific 69572).

2. These dialysis units are then placed in 200 ml of TE buffer containing 2 M KCl, and slowly dialyzed with a linear gradient into TE with 10 mM KCl at 4° C. After 16 – 18 h samples are removed from micro-dialysis units and centrifuged at 15'000 rcf for 10 minutes at 4° C to remove aggregates. The supernatant is removed and the concentration measured using a UV spectrometer.

3. To determine the saturation of chromatin arrays, 100 ng of arrays (6 - 7 fmoles) are taken for ScaI (NEB 3122) digestion using 20 units of enzyme in 1x Cutsmart buffer. This digestion reaction is performed in 20 ul at 37° C for 2 h. The digestion is analyzed on 5 % TBE polyacrylamide gels on ice ran at 150 V for 50 mins, to see the formation of MMTV nucleosomes and the disappearance of the free 1 x 601 DNA band. As MMTV has a lower propensity to form nucleosomes, the appearance of MMTV nucleosomes indicate that all 1 x 601 sites have been filled.

4.7 Flow chamber construction and assembly

Careful cleaning (**Fig 4a**), silanization and PEGylation of coverslips and glass slides is vital to ensure the reduction of background fluorescence during single molecule experiments. Here we describe a method using H_2SO_4 and H_2O_2 as etching reagents [18] (12 slides are usually made at a time).

1. Using a drill press equipped with a diamond coated drill bit (0.75 mm thickness), a total of 8 holes organized in 2 columns (24 mm from the short edge, 5 mm from the long edge and thus each column is 28 mm apart) and 4 rows (each separated by 5 mm) are drilled into each glass slide (76 x 26 mm) (**Fig 4b**).

2. Glass slides containing drilled holes, along with coverslips (24 x 40 mm, 1.5mm thickness) are placed in glass staining jars filled with a 10 % w/v solution of Alconox detergent (Merck, 242985). The staining jars are then placed in a sonicator filled with water and sonicated at room temperature for 20 minutes. The detergent solution is discarded and glass slides as well as coverslips are washed abundantly with ultra-pure water.

3. Glass slides and coverslips are then submerged in acetone and the sonication is repeated. The acetone is discarded and glass slides as well as coverslips are washed abundantly with ultra-pure water.

4. Glass slides and coverslips are then submerged in ethanol and the sonication is repeated a final time. The ethanol is discarded and glass slides as well as coverslips are washed abundantly with ultra-pure water (It is possible to keep glass slides and cover slips overnight in ultra-pure water at this stage).

5. In clean glass staining jars placed in an ice bath under the hood, a mixture of 25 % H_2O_2 (30% H_2O_2) and 75 % H_2SO_4 (this is called piranha solution) is prepared by slow dropwise addition of H_2O_2 to H_2SO_4. This solution should be gently mixed using a metal spatula at regular intervals during H_2O_2 addition. Glass slides and coverslips are transferred from glass staining jars containing ultra-pure water into the glass staining jars containing piranha solution. Coverslips should be fully submerged, whereas only the area between the drilled holes on glass slides should be covered. The etching process is left for minimum 1 hour. After which all coverslips and glass slides are transferred to clean glass staining jars and washed abundantly with ultra-pure water.

6. Glass slides and coverslips are then submerged in acetone and the sonicated for 10 mins. For passivation, a 2% solution of (3-Aminopropyl)triethoxysilane (APTES) in acetone is prepared, cover slips and glass slides are submerged and incubated for 5 minutes. Coverslips and glass slides are transferred to clean glass staining jars and washed abundantly with ultra-pure water.

7. For 12 flow chambers, 60 strips made of double-sided SecureSeal adhesive tape (Sigma 620001) of 4.5 cm x 3 mm are required. Glass slides and coverslips are dried with nitrogen gas before 5 strips of adhesive tape are applied to the glass slides to create 4 channels each containing 2 predrilled holes. Gently, the dried coverslip is aligned over the adhesive tape strips, with an extra length of adhesive tape extending out on both sides of the coverslip. Finally, rapid curing two-component epoxy resin (Devcon® 5-minute epoxy) is applied to the short edge of the coverslip. At this stage the resin can be seen entering the channel, this is the reason why the tape strips should be applied as such that they extend beyond the predrilled

holes. At this stage flow chambers can be placed individually in 50 ml plastic tubes and kept in a vacuumed packed plastic at -20° C.

8. On the day of use, flow chambers are taken out of the -20° C to thaw and plastic pipette tips (4 x 200 µl and 4 x 20 µl) are epoxy glued into individual drilled holes to create buffer reservoirs and outlets. Once the epoxy has hardened, 50 µl of a mixture of 40 mg of MPEG SVA-5000 (Laysanbio M-SVA-5K) and 1 mg of Biotin-PEG- SVA-5000 (Laysanbio Bio-SVA-5K) in 0.1 M Sodium tetraborate pH 8.5 (Sigma S9640) is injected into each microchannel. This solution is left to passivate for at least 3 h.

4.8 Imaging buffer

For imaging buffer, a 4mM stock of (±)-6-Hydroxy-2,5,7,8-tetramethylchromane-2-carboxylic acid (Trolox) (Sigma 238813) is prepared by dissolving 30 mg Trolox in 30 ml of degassed ultrapure water. The pH is adjusted to 8.0 (this step is difficult as Trolox does not dissolve easily, however pH is readjusted at a later step). This stock is left shaking overnight in the dark (for 12 – 16 h) and later filtered using 0.2 µm filter and a UV absorption in UV-VIS (290 nm) in a 1:50 solution (ε = 2350 ± 100 M^{-1} cm^{-1}) is taken. The stock solution is completed to make 4 mM and pH is readjusted if necessary. Completed imaging buffer (IB) consists of 50 mM HEPES (Sigma H3375) pH 7.5, 130 mM KCl (Sigma 60130), 10% v/v glycerol (Fischer BP350-1), 0.005% v/v Tween 20 (Applichem A7564), 2 mM Trolox and 3.2% w/v glucose (Fischer BP350-1). This can be aliquoted into 1 ml stocks, frozen and only when required, defrosted and used within 2 h. As an oxygen scavenging system, Bovine liver catalase (Sigma C40) and glucose oxidase from *Aspergillus niger* Type VII (Sigma G2133) was chosen (GODCAT). To make a 100 x stock of GODCAT, 1 mg of Catalase is dissolved into 100 µl of 50 mM Phosphate buffer pH 7. 20 µl of this solution is taken and added to 30 µl of T50 (10 mM Tris-HCl, pH 8.5 and 50 mM NaCl). This solution is used to dissolve 5 mg of Glucose oxidase, note that this oxygen scavenging system can be kept at 4° C for 7 days and remain active. Additionally, 0.1 – 2 mg/ml BSA can be incubated in microchannels and supplemented in all buffers used.

4.9 Imaging conditions

4.9.1 Washing microchannels

PTFE tubing (Fischer 11929445) is cut and placed (not glued) into a microchannel reservoir on one end and on the other a 1ml syringe with a needle is placed in a syringe pump (WPI INC). The draw speed for the syringe pump is set to 500 µl/min. All buffers and samples are applied to the opposite reservoir of the same microchannel using 1 ml syringes with needles.

When required individual microchannels are washed with 500 µl ultrapure water followed by 500 µl of T50 (10 mM Tris-HCl, pH 8.5 and 50 mM NaCl). Neutravidin solutions of 0.2 mg/ml are dissolved in T50 buffer and incubated for 5 mins, after which excess neutravidin is washed using 500 µl T50.

4.9.2 Measuring background fluorescence

Background fluorescence is measured using both 532 nm and 657 nm excitation. For this a 1-minute movie was taken using continuous illumination (camera settings: t_{on} 100 msecs and t_{off} 0.32 msecs) of the glass surface. Laser power was set to 0.8 – 1 mW as measured by power meter (Newport 843-R) at the objective. Movies for 532 nm and 647 nm are taken at different locations in the microchannels. If high background is visible in microchannels they are discarded at this stage.

4.9.3 Loading of labelled chromatin arrays and addition of Rap1

Microchannels are washed as in section **4.8.1** and Alexa 647 labelled chromatin arrays are diluted to 100 pM in imaging buffer to a total volume of 99 µl and 1 µl 100x GODCAT is added. This solution is injected into the washed microchannel, note this process can be followed using continuous illumination (camera settings: t_{on} 100 msecs and t_{off} 0.32 msecs) to see density of arrays on surface in real time. In a region of interest (ROI) of 50 µm x 25 µm the ideal density is between 200 – 300 spots. This allows for separation and detection of single chromatin arrays, but at the same time provides an adequate number of events even in the case where chromatin arrays have 2 or 3 binding events within the imaging time. Excess unbound chromatin arrays are washed with 500 µl T50. Finally, effector protein is diluted to 50 – 100 pM in 99 µl of IB buffer supplemented with 1 µl 100x GODCAT. ~30 µl of this solution is washed through the microchannel at 500 µl/min, the flow rate is then set to 0.5 µl/min during data acquisition. Depending on the kinetic behavior observed, laser illumination and camera settings can be modulated to minimize photobleaching.

Acknowledgments

This work was supported by the Swiss National Science foundation (SNSF, grant 31003A_173169), the Ecole polytechnique fédérale (EPFL) and the NCCR Chemical Biology.

References

[1] K. van Holde, Chromatin, Springer, New York, 1989.

[2] K. Luger, A.W. Mader, R.K. Richmond, D.F. Sargent, T.J. Richmond, Crystal structure of the nucleosome core particle at 2.8 A resolution, Nature, 389 (1997) 251-260.

[3] J. Widom, A relationship between the helical twist of DNA and the ordered positioning of nucleosomes in all eukaryotic cells, Proc Natl Acad Sci U S A, 89 (1992) 1095-1099.

[4] T. Schalch, S. Duda, D.F. Sargent, T.J. Richmond, X-ray structure of a tetranucleosome and its implications for the chromatin fibre, Nature, 436 (2005) 138-141.

[5] F. Song, P. Chen, D. Sun, M. Wang, L. Dong, D. Liang, R.M. Xu, P. Zhu, G. Li, Cryo-EM study of the chromatin fiber reveals a double helix twisted by tetranucleosomal units, Science, 344 (2014) 376-380.

[6] I. Garcia-Saez, H. Menoni, R. Boopathi, M.S. Shukla, L. Soueidan, M. Noirclerc-Savoye, A. Le Roy, D.A. Skoufias, J. Bednar, A. Hamiche, D. Angelov, C. Petosa, S. Dimitrov, Structure of an H1-Bound 6-Nucleosome Array Reveals an Untwisted Two-Start Chromatin Fiber Conformation, Mol Cell, (2018).

[7] S. Kilic, S. Felekyan, O. Doroshenko, I. Boichenko, M. Dimura, H. Vardanyan, L.C. Bryan, G. Arya, C.A.M. Seidel, B. Fierz, Single-molecule FRET reveals multiscale chromatin dynamics modulated by HP1alpha, Nat Commun, 9 (2018) 235.

[8] B.D. Strahl, C.D. Allis, The language of covalent histone modifications, Nature, 403 (2000) 41-45.

[9] K. Luger, M.L. Dechassa, D.J. Tremethick, New insights into nucleosome and chromatin structure: an ordered state or a disordered affair?, Nat. Rev. Mol. Cell. Biol., 13 (2012) 436-447.

[10] S.D. Taverna, H. Li, A.J. Ruthenburg, C.D. Allis, D.J. Patel, How chromatin-binding modules interpret histone modifications: lessons from professional pocket pickers, Nat Struct Mol Biol, 14 (2007) 1025-1040.

[11] A.J. Ruthenburg, H. Li, D.J. Patel, C.D. Allis, Multivalent engagement of chromatin modifications by linked binding modules, Nat Rev Mol Cell Biol, 8 (2007) 983-994.

[12] C.R. Clapier, B.R. Cairns, The Biology of Chromatin Remodeling Complexes, Ann. Rev. Biochem., 78 (2009) 273-304.

[13] W.K.M. Lai, B.F. Pugh, Understanding nucleosome dynamics and their links to gene expression and DNA replication, Nat Rev Mol Cell Biol, 18 (2017) 548-562.

[14] D.M. Presman, D.A. Ball, V. Paakinaho, J.B. Grimm, L.D. Lavis, T.S. Karpova, G.L. Hager, Quantifying transcription factor binding dynamics at the single-molecule level in live cells, Methods, 123 (2017) 76-88.

[15] R. Tatavosian, H.N. Duc, T.N. Huynh, D. Fang, B. Schmitt, X. Shi, Y. Deng, C. Phiel, T. Yao, Z. Zhang, H. Wang, X. Ren, Live-cell single-molecule dynamics of PcG proteins imposed by the DIPG H3.3K27M mutation, Nat Commun, 9 (2018) 2080.

[16] C.Y. Zhen, R. Tatavosian, T.N. Huynh, H.N. Duc, R. Das, M. Kokotovic, J.B. Grimm, L.D. Lavis, J. Lee, F.J. Mejia, Y. Li, T. Yao, X. Ren, Live-cell single-molecule tracking reveals co-recognition of H3K27me3 and DNA targets polycomb Cbx7-PRC1 to chromatin, eLife, 5 (2016).

[17] D.T. Youmans, J.C. Schmidt, T.R. Cech, Live-cell imaging reveals the dynamics of PRC2 and recruitment to chromatin by SUZ12-associated subunits, Genes Dev, 32 (2018) 794-805.

[18] Y. Wang, L. Guo, I. Golding, E.C. Cox, N.P. Ong, Quantitative transcription factor binding kinetics at the single-molecule level, Biophys J, 96 (2009) 609-620.

[19] Y. Luo, J.A. North, S.D. Rose, M.G. Poirier, Nucleosomes accelerate transcription factor dissociation, Nucleic Acids Res., 42 (2014) 3017-3027.

[20] B.T. Donovan, H. Chen, C. Jipa, L. Bai, M.G. Poirier, Dissociation rate compensation mechanism for budding yeast pioneer transcription factors, eLife, 8 (2019).

[21] S. Kilic, A.L. Bachmann, L.C. Bryan, B. Fierz, Multivalency governs HP1alpha association dynamics with the silent chromatin state, Nat. Commun., 6 (2015) 7313.

[22] J. Choi, A.L. Bachmann, K. Tauscher, C. Benda, B. Fierz, J. Muller, DNA binding by PHF1 prolongs PRC2 residence time on chromatin and thereby promotes H3K27 methylation, Nat Struct Mol Biol, (2017).

[23] R.K. McGinty, S. Tan, Nucleosome Structure and Function, Chemical Reviews, 115 (2015) 2255-2273.

[24] R. Simpson, D. Stafford, Structural features of a phased nucleosome core particle, Proc Natl Acad Sci U S A, 80 (1983) 51-55.

[25] P.T. Lowary, J. Widom, New DNA sequence rules for high affinity binding to histone octamer and sequence-directed nucleosome positioning, J. Mol. Biol., 276 (1998) 19-42.

[26] K. Struhl, E. Segal, Determinants of nucleosome positioning, Nat Struct Mol Biol, 20 (2013) 267-273.

[27] A. Flaus, Principles and practice of nucleosome positioning in vitro, Front Life Sci, 5 (2011) 5-27.

[28] N. Krietenstein, M. Wal, S. Watanabe, B. Park, C.L. Peterson, B.F. Pugh, P. Korber, Genomic Nucleosome Organization Reconstituted with Pure Proteins, Cell, 167 (2016) 709-721 e712.

[29] N. Kaplan, I.K. Moore, Y. Fondufe-Mittendorf, A.J. Gossett, D. Tillo, Y. Field, E.M. LeProust, T.R. Hughes, J.D. Lieb, J. Widom, E. Segal, The DNA-encoded nucleosome organization of a eukaryotic genome, Nature, 458 (2009) 362-366.

[30] E. Segal, Y. Fondufe-Mittendorf, L. Chen, A. Thastrom, Y. Field, I.K. Moore, J.P. Wang, J. Widom, A genomic code for nucleosome positioning, Nature, 442 (2006) 772-778.

[31] M. Li, M.D. Wang, Unzipping Single DNA Molecules to Study Nucleosome Structure and Dynamics, Nucleosomes, Histones & Chromatin, Pt B, 513 (2012) 29-58.

[32] T.T. Ngo, Q. Zhang, R. Zhou, J.G. Yodh, T. Ha, Asymmetric unwrapping of nucleosomes under tension directed by DNA local flexibility, Cell, 160 (2015) 1135-1144.

[33] J.A. North, J.C. Shimko, S. Javaid, A.M. Mooney, M.A. Shoffner, S.D. Rose, R. Bundschuh, R. Fishel, J.J. Ottesen, M.G. Poirier, Regulation of the nucleosome unwrapping rate controls DNA accessibility, Nucleic Acids Res, 40 (2012) 10215-10227.

[34] B. Dorigo, T. Schalch, A. Kulangara, S. Duda, R.R. Schroeder, T.J. Richmond, Nucleosome arrays reveal the two-start organization of the chromatin fiber, Science, 306 (2004) 1571-1573.

[35] M.G. Poirier, E. Oh, H.S. Tims, J. Widom, Dynamics and function of compact nucleosome arrays, Nat. Struct. Mol. Biol., 16 (2009) 938-944.

[36] D.R. Banerjee, C.E. Deckard, 3rd, M.B. Elinski, M.L. Buzbee, W.W. Wang, J.D. Batteas, J.T. Sczepanski, Plug-and-Play Approach for Preparing Chromatin Containing Site-Specific DNA Modifications: The Influence of Chromatin Structure on Base Excision Repair, J Am Chem Soc, 140 (2018) 8260-8267.

[37] M.M. Muller, B. Fierz, L. Bittova, G. Liszczak, T.W. Muir, A two-state activation mechanism controls the histone methyltransferase Suv39h1, Nat Chem Biol, 12 (2016) 188-193.

[38] R. Roy, S. Hohng, T. Ha, A practical guide to single-molecule FRET, Nat Methods, 5 (2008) 507-516.

[39] G.T. Dempsey, J.C. Vaughan, K.H. Chen, M. Bates, X. Zhuang, Evaluation of fluorophores for optimal performance in localization-based super-resolution imaging, Nat Methods, 8 (2011) 1027-1036.

[40] J.B. Grimm, B.P. English, J. Chen, J.P. Slaughter, Z. Zhang, A. Revyakin, R. Patel, J.J. Macklin, D. Normanno, R.H. Singer, T. Lionnet, L.D. Lavis, A general method to improve fluorophores for live-cell and single-molecule microscopy, Nat Methods, 12 (2015) 244-250, 243 p following 250.

[41] L. Wang, A. Brock, B. Herberich, P.G. Schultz, Expanding the genetic code of Escherichia coli, Science, 292 (2001) 498-500.

[42] D. Nguyen, M. Garcia Alai, S. Virdee, J. Chin, Genetically directing ε-N, N-dimethyl-L-lysine in recombinant histones, Chem Biol, 17 (2010) 1072-1076.

[43] M.D. Simon, F.X. Chu, L.R. Racki, C.C. de la Cruz, A.L. Burlingame, B. Panning, G.J. Narlikar, K.M. Shokat, The site-specific installation of methyl-lysine analogs into recombinant histones, Cell, 128 (2007) 1003-1012.

[44] P.E. Dawson, T.W. Muir, I. Clark-Lewis, S.B.H. Kent, Synthesis of proteins by native chemical ligation, Science, 266 (1994) 776-779.

[45] T.W. Muir, D. Sondhi, P.A. Cole, Expressed protein ligation: a general method for protein engineering, Proc Natl Acad Sci U S A, 95 (1998) 6705-6710.

[46] Q. Wan, S.J. Danishefsky, Free-radical-based, specific desulfurization of cysteine: A powerful advance in the synthesis of polypeptides and glycopolypeptides, Angew Chem Int Ed Engl, 46 (2007) 9248-9252.

[47] L.Z. Yan, P.E. Dawson, Synthesis of peptides and proteins without cysteine residues by native chemical ligation combined with desulfurization, J Am Chem Soc, 123 (2001) 526-533.

[48] S. Kilic, I. Boichenko, C.C. Lechner, B. Fierz, A bi-terminal protein ligation strategy to probe chromatin structure during DNA damage, Chem Sci, 9 (2018) 3704-3709

[49] C.C. Lechner, N.D. Agashe, B. Fierz, Traceless Synthesis of Asymmetrically Modified Bivalent Nucleosomes, Angew Chem Int Ed Engl, 55 (2016) 2903-2906.

[50] J.A. Camarero, T.W. Muir, Native chemical ligation of polypeptides, Curr Protoc Protein Sci, Chapter 18 (2001) Unit18 14.

[51] J.B. Blanco-Canosa, P.E. Dawson, An efficient Fmoc-SPPS approach for the generation of thioester peptide precursors for use in native chemical ligation, Angew Chem Int Ed Engl, 47 (2008) 6851-6855.

[52] G.M. Fang, Y.M. Li, F. Shen, Y.C. Huang, J.B. Li, Y. Lin, H.K. Cui, L. Liu, Protein chemical synthesis by ligation of peptide hydrazides, Angew Chem Int Ed Engl, 50 (2011) 7645-7649.

[53] R.E. Thompson, X. Liu, N. Alonso-Garcia, P.J. Pereira, K.A. Jolliffe, R.J. Payne, Trifluoroethanethiol: an additive for efficient one-pot peptide ligation-desulfurization chemistry, J Am Chem Soc, 136 (2014) 8161-8164.

[54] Y.C. Huang, C.C. Chen, S. Gao, Y.H. Wang, H. Xiao, F. Wang, C.L. Tian, Y.M. Li, Synthesis of l- and d-Ubiquitin by One-Pot Ligation and Metal-Free Desulfurization, Chemistry, 22 (2016) 7623-7628.

[55] P.N. Dyer, R.S. Edayathumangalam, C.L. White, Y. Bao, S. Chakravarthy, U.M. Muthurajan, K. Luger, Reconstitution of nucleosome core particles from recombinant histones and DNA, Methods Enzymol, 375 (2004) 23-44.

[56] L.M. Carruthers, C. Tse, K.P. Walker, 3rd, J.C. Hansen, Assembly of defined nucleosomal and chromatin arrays from pure components, Methods Enzymol, 304 (1999) 19-35.

[57] B. Dorigo, T. Schalch, K. Bystricky, T.J. Richmond, Chromatin fiber folding: requirement for the histone H4 N-terminal tail, J Mol Biol, 327 (2003) 85-96.

[58] Y. Zhang, K.Y. Park, K.F. Suazo, M.D. Distefano, Recent progress in enzymatic protein labelling techniques and their applications, Chem Soc Rev, 47 (2018) 9106-9136.

[59] N.H. Shah, T.W. Muir, Inteins: Nature's Gift to Protein Chemists, Chem Sci, 5 (2014) 446-461.

[60] A. Keppler, S. Gendreizig, T. Gronemeyer, H. Pick, H. Vogel, K. Johnsson, A general method for the covalent labeling of fusion proteins with small molecules in vivo, Nat Biotechnol, 21 (2003) 86-89.

[61] P.R. Selvin, T. Ha, Single-Molecule Techniques: A Laboratory Manual, Cold Spring Harbor Laboratory Press, 2008.

[62] E.M. Kudalkar, Y. Deng, T.N. Davis, C.L. Asbury, Coverslip Cleaning and Functionalization for Total Internal Reflection Fluorescence Microscopy, Cold Spring Harbor protocols, 2016 (2016).

[63] M.T. Hoffman, J. Sheung, P.R. Selvin, Fluorescence imaging with one nanometer accuracy: in vitro and in vivo studies of molecular motors, Methods Mol Biol, 778 (2011) 33-56.

[64] T. Ha, I. Rasnik, W. Cheng, H.P. Babcock, G.H. Gauss, T.M. Lohman, S. Chu, Initiation and re-initiation of DNA unwinding by the Escherichia coli Rep helicase, Nature, 419 (2002) 638-641.

[65] L. Schermelleh, A. Ferrand, T. Huser, C. Eggeling, M. Sauer, O. Biehlmaier, G.P.C. Drummen, Super-resolution microscopy demystified, Nat Cell Biol, 21 (2019) 72-84.

[66] A. Allahverdi, R. Yang, N. Korolev, Y. Fan, C. Davey, C.-F. Liu, L. Nordenskiöld, The effects of histone H4 tail acetylations on cation-induced chromatin folding and self-association, Nucleic Acids Res, 39 (2011) 1680-1691.

[67] C.E. Aitken, R.A. Marshall, J.D. Puglisi, An oxygen scavenging system for improvement of dye stability in single-molecule fluorescence experiments, Biophys J, 94 (2008) 1826-1835.

[68] J. Vogelsang, R. Kasper, C. Steinhauer, B. Person, M. Heilemann, M. Sauer, P. Tinnefeld, A reducing and oxidizing system minimizes photobleaching and blinking of fluorescent dyes, Angew Chem Int Ed Engl, 47 (2008) 5465-5469.

[69] W. Gong, P. Das, S. Samanta, J. Xiong, W. Pan, Z. Gu, J. Zhang, J. Qu, Z. Yang, Redefining the photo-stability of common fluorophores with triplet state quenchers: mechanistic insights and recent updates, Chemical communications, 55 (2019) 8695-8704.

[70] R.B. Altman, Q. Zheng, Z. Zhou, D.S. Terry, J.D. Warren, S.C. Blanchard, Enhanced photostability of cyanine fluorophores across the visible spectrum, Nat Methods, 9 (2012) 428-429.

[71] R. Dave, D.S. Terry, J.B. Munro, S.C. Blanchard, Mitigating unwanted photophysical processes for improved single-molecule fluorescence imaging, Biophys J, 96 (2009) 2371-2381.

[72] W.S. Rasband, ImageJ, U.S. National Institutes of Health, Bethesda, Maryland, USA, https://imagej.nih.gov/ij/ (1997-2018).

[73] S.H. Chung, R.A. Kennedy, Forward-backward non-linear filtering technique for extracting small biological signals from noise, Journal of neuroscience methods, 40 (1991) 71-86.

[74] T. Aggarwal, D. Materassi, R. Davison, T. Hays, M. Salapaka, Detection of Steps in Single Molecule Data, Cellular and molecular bioengineering, 5 (2012) 14-31.

[75] L.C. Bryan, D.R. Weilandt, A.L. Bachmann, S. Kilic, C.C. Lechner, P.D. Odermatt, G.E. Fantner, S. Georgeon, O. Hantschel, V. Hatzimanikatis, B. Fierz, Single-molecule kinetic analysis of HP1-chromatin binding reveals a dynamic network of histone modification and DNA interactions, Nucleic Acids Res., (2017).

[76] S.A. McKinney, C. Joo, T. Ha, Analysis of single-molecule FRET trajectories using hidden Markov modeling, Biophys J, 91 (2006) 1941-1951.